Comparison of the Surface Properties of the Assembled Silver Nanoparticle Electrode and Roughened Silver Electrode

Junwei Zheng,*,† Xiaowei Li,† Renao Gu,† and Tianhong Lu‡

Department of Chemistry, Suzhou University, Suzhou 215006, P.R. China, and Department of Chemistry, Nanjing Normal University, Nanjing 210097, P. R. China.

Received: May 31, 2001; In Final Form: October 15, 2001

Surface properties of an assembled silver nanoparticle/ITO (AAgNP/ITO) electrode and an electrochemically roughened Ag electrode were studied by surface-enhanced Raman spectroscopy and electrochemical techniques. Methyl viologen (MV) and p-aminothiophenol (PATP) were used as the probing molecules. The electrochemical results show that MV can be strongly adsorbed on the surface of the roughened Ag electrode but not on the surface of the AAgNP/ITO electrode. The SERS spectra further indicate that the MV molecules are adsorbed with parallel orientation to the surface of the roughened Ag electrode. The fact that no SERS spectrum was observed on the AAgNP/ITO electrode may imply that there are no required active sites on the surface of the isolated Ag nanoparticle for the interaction between the ring plane of MV and Ag nanoparticle. On the other hand, the SERS spectra of PATP reveal that PATP molecules can be adsorbed on the surfaces of both electrodes, because of the perpendicular orientation of the adsorbed molecules relative to the surface of the Ag nanoparticle on the electrodes. Nevertheless, changes in relative intensities of several a_1 and b_2 modes also indicate that there are slight differences in the orientation of the adsorbed PATP and the chemical property of the electrode surfaces.

Introduction

Since the first discovery of the surface enhancement effect of Raman scattering of pyridine on a roughened silver electrode, surface-enhanced Raman scattering (SERS) has proven to be a powerful method in research and applications in the field of analytical chemistry, biochemistry, and catalysis.[1−6] In general, appreciable enhancement of Raman scattering can only be obtained on the surfaces of certain metals, such as Au, Ag, and Cu. More importantly, to gain efficient enhancement, it is also necessary to create both large scale and atomic scale roughness on metal surfaces, which enable surface plasmons to resonate with the light at the irradiation wavelength. Except for the fact that the basic mechanism of SERS is still under debate, considerable effort has been devoted to searching for better SERS substrates both for fundamental interests and practical applications.[7−15] Electrochemically roughened electrode surfaces and metal colloids are the most commonly used SERS substrates in various research works. In principle, the electrochemical roughening procedure endows the electrode surface with nanosized metal particles, which are comparable to those in the corresponding metal colloid solution. Although it has been recognized that the surface properties of nanostructured metal particles are critical for the enhancement of the SERS signal, a direct comparison of the surface property of an electrochemically roughened electrode to that of the metal particle in colloid solution is difficult, mainly because of the random movement of the particles in colloid solution. Recently, nanostructured metal particles have been assembled in such a highly ordered manner that the particles form a two-dimensional structure on the surfaces of substrates, such as glass, silicon, etc.[16−19] This undoubtedly provides an excellent system for making a direct comparison of nanostructured metal particles with those formed on an electrochemically roughened metal electrode. This is also a promising approach to selectively probe the effect of the nature of the particles and interactions between particles on Raman scattering of the adsorbed species. Moreover, such metal nanoparticle assembled electrodes have been shown to have some unique properties, i.e., an improved heterogeneous rate constant for electron transfer to $[Ru(NH_3)_6]^{3+}$ on a Ag colloid deposited carbon electrode.[16]

In this paper, the surface properties of a silver nanoparticle array/ITO electrode (AAgNP/ITO) and an electrochemically roughened Ag electrode were investigated with methyl viologen (MV) and p-aminothiophenol (PATP) as the probing molecules, using surface-enhanced FT-Raman spectroscopy (FT-SERS) and electrochemical techniques. We found that the electrochemical and FT-SERS spectroscopic behaviors of the probing molecules critically depend on the nanoscaled surface features of the electrodes.

Experimental Section

Chemicals. Methyl viologen dichloride (MV^{2+}), PATP, and poly-L-lysine were purchased from Sigma Chemical Co. and used without further purification. The other chemicals are all reagent grade. All of the solutions were prepared with Millipore water. The solutions used for the electrochemical measurements were 0.5 mM MV^{2+} containing 0.1 M Na_2SO_4. To remove the oxygen dissolved in the solutions, the solutions were bubbled with purified nitrogen for 30 min prior to the measurements.

Apparatus and Methods. The electrochemical measurements were performed on a CHI-660 electrochemical station connected with a PC computer. A conventional three-electrode electro-

* To whom correspondence should be addressed. Phone: (86)512−5112645. Fax: (86)512-5321918. E-mail: jwzheng@suda.edu.cn.
† Suzhou University.
‡ Nanjing Normal University.

10.1021/jp012083r CCC: $22.00
Published on Web 01/11/2002

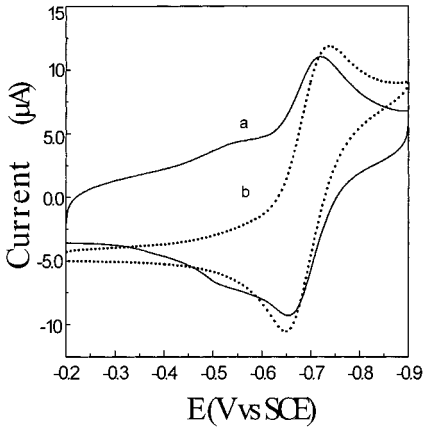

Figure 1. Cyclic voltammograms of MV in 0.1 M Na_2SO_4 solution (a) at the roughened Ag electrode and (b) at the AAgNP/ITO electrode.

chemical cell was used in all measurements. A platinum wire was used as the auxiliary electrode. A saturated calomel electrode (SCE) served as the reference electrode. All of the potentials were reported with respect to SCE.

The Ag electrode used as the working electrode was constructed from a polycrystalline plate sealed in glass tubing with Torr Seal (Vaian). The electrode surface was sequentially polished with 5.0, 0.3, and 0.05 um alumina/water slurries until a shiny, mirrorlike finish was obtained. It was then sonicated twice in Millipore water and washed thoroughly with Millipore water. Then, the polished Ag electrode was roughened using a double-potential step oxidation−reduction cycle (ORC) in a 0.1 M KCl solution. This consisted of a double potential step from −0.40 to +0.25 V, where a 250 μC charge was passed. Then, the electrode potential was stepped back to −0.40 V until the current reached a minimum.

A silver colloid solution was prepared by reducing $AgNO_3$ with citrate according to the protocol in the literature.[20] The maximum of the electronic absorption of the colloid solution was at ca. 420 nm. The AAgNP/ITO electrode was prepared as follows: The surface of an ITO electrode was first modified with a layer of poly-L-lysine by dipping the ITO electrode into a 0.5% poly-L-lysine solution for 2 h. The modified electrode was then thoroughly washed with water and dipped into a silver colloid solution overnight. After this self-assembling process, the electrode surface was covered with a layer of Ag particles.

The Raman instrument included a FT-Raman spectrometer (Nicolet 960) equipped with a liquid-nitrogen-cooled Ge detector and a Nd/VO_4 laser (1064 nm) as an excitation source. The laser power used was about 100 mW at the samples. The resolution of the Raman instrument was ca. 4 cm^{-1} at the excitation wavelength used here. The scattered light was collected in a backscattering geometry. Scanning electron micrographs were obtained using a Hitachi 7350G SEM microscope.

Results and Discussion

Methylviologen dication (MV^{2+}) can be strongly adsorbed on the surface of a roughened Ag electrode surface, and consequently, the redox reactions of adsorbed MV^{2+} occur at more positive potential than that of the solution species.[21,22] This is clearly shown in cyclic voltammograms (CVs) in Figure 1a. In the potential region, two pairs of redox peaks were observed. The oxidation and reduction peaks of the first pair are located at −0.53 and −0.55 V, respectively, and the peak current is proportional to the scan rate. This pair of redox peaks is ascribed to be the result of the one-electron redox reactions of adsorbed MV^{2+}.[21,22] The second pair of redox peaks appears at a more negative potential with an oxidation peak at −0.66 V and the reduction peak at −0.72 V, respectively. The peak currents vary linearly with the square root of the scan rate, indicating a diffusion-controlled electrode process. Obviously, this corresponds to the one-electron redox reactions of MV^{2+} in solution. Under the same experimental conditions, the CV measurement of MV was also performed for the AAgNP/ITO electrode. To our surprise, only one pair of peaks corresponding to the redox reactions of solution species was observed, as shown in Figure 1b. Thus, it seems that the nanostructured Ag particles assembled in an ordered manner in this particular case do not provide the efficient active sites for the adsorption of MV^{2+} molecules.

The above results clearly suggest that although the nanostructured Ag particles or the roughness feature may be formed on the Ag electrode surface during the electrochemical roughening process, the relative differences in surface properties to that of the AAgNP/ITO electrode could result in the difference in electrode behaviors of MV^{2+}. Possible difference in morphology of the surfaces of two electrodes were considered first. Direct evidence of the difference in morphology of the electrodes comes from the scanning electron microscopy study, as illustrated in Figure 2. On the surface of the roughened Ag electrode, there are small particles with a quite wide size distribution and random arrangement (Figure 2A). Importantly, some relatively large surface defects and aggregates of the Ag nanoparticles formed by electrochemical roughening were observed on the electrode surface. On the other hand, the nanostructured Ag particles assembled on ITO electrode surface show a highly ordered arrangement with two-dimensional submonolayer structure (Figure 2B). The average size of the particles is ca. 100 nm, and the distance between the particles approximates to the particle size. Most of the Ag particles exist separately, but aggregates consisting of two or three particles were also observed in the structure. It should be pointed out that the real sizes of the Ag nanoparticles should be smaller, because of the additional layer of gold deposited in the sample pretreatment procedure prior to the SEM measurements. It is obvious that the major differences in the surface morphologies of the two electrodes are the particle arrangement and the large scale surface features such as surface defects and aggregation of Ag particles which at first glance may play a critical role on MV^{2+} adsorption.

To determine the trait of adsorption of MV, the FT-SERS spectra of MV^{2+} were measured for both electrodes, and the results are shown in Figure 3. For comparison, the normal Raman spectrum of solid MV is also presented. A number of researchers have investigated the SERS of MV and its reduced forms on both the electrochemically roughened Ag electrode and Ag colloid, and different types of adsorption and photoinduced reduction or degradation have been reported, because of the high energy of excitation in visible region used in most of the studies.[21−24] In the present study, a 1064 nm excitation used could efficiently avoid photoinduced reduction and degradation of MV. Compared to the solid spectrum (Figure 3a), the most notable differences in FT-SERS spectrum of MV^{2+} on the surface of roughened Ag electrode (Figure 3b) are frequency shifts and changes in relative intensity for most of the bands. The stretching modes related to the N heteroatom, ν(C−N) and ν(N−CH_3), shift from 1555 and 1202 cm^{-1} to 1536 and 1193 cm^{-1}, respectively; the band of the ring C−C stretching, $\nu(C-C)_r$, also shifts from 1657 to 1648 cm^{-1} and tremendously increases in relative intensity; the interring C−C vibration, $\nu(C-C)_{ir}$, at 1303 cm^{-1} is more intense than ν(N−CH_3) in Figure

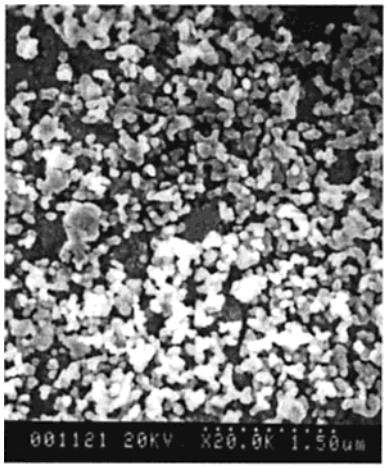

(A)

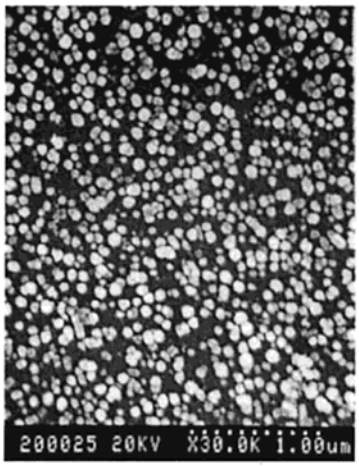

(B)

Figure 2. SEM graphs of the electrode surfaces: (A) the roughened Ag electrode and (B) the AAgNP/ITO electrode.

3a, where it appears at 1294 cm^{-1}, and its intensity is comparable to that of $\nu(N-CH_3)$ in the FT-SERS spectrum (Figure 3b). These large frequency shifts of the bands related to the C−N and C−C bonds suggest that there are strong interactions between those chemical bonds and the surface of the metal. Thus, the adsorbed MV^{2+} could adopt a parallel orientation to the electrode surface, where two nitrogen atoms in MV^{2+} are directly bound to the electrode surface. In fact, the SERS spectrum is similar to the type II SERS spectrum of MV^{2+} reported by Cotton et al.,[21] who suggested that a surface complex of MV, the counterion, and silver ion or silver atom cluster is probably formed on the electrode surface. The SERS spectrum is mainly from the chemical enhancement. The enhanced modes in the SERS spectrum belong to the symmetric fundamental vibrations. In general, the charge transfer (CT) process would enhance the symmetrical modes, preferentially the modes involving the vibrational coordinates which are relaxed by the electronic excited state.[25] A similar spectrum was also reported by Wu et al.[26] On the basis of the calculation of the bond polarizability derivative of MV, they concluded that the adsorption configuration of MV is flat on the roughened silver electrode. In contrast, on the surface of the AAgNP/ITO electrode, only very weak SERS bands were observed (data not shown), confirming that MV^{2+} was not adsorbed on the surface of the electrode. The weak SERS single may result from MV^{2+} adsorbed on the aggregate of Ag particles as those demonstrated in Figure 2B. On the basis of the experimental results, we

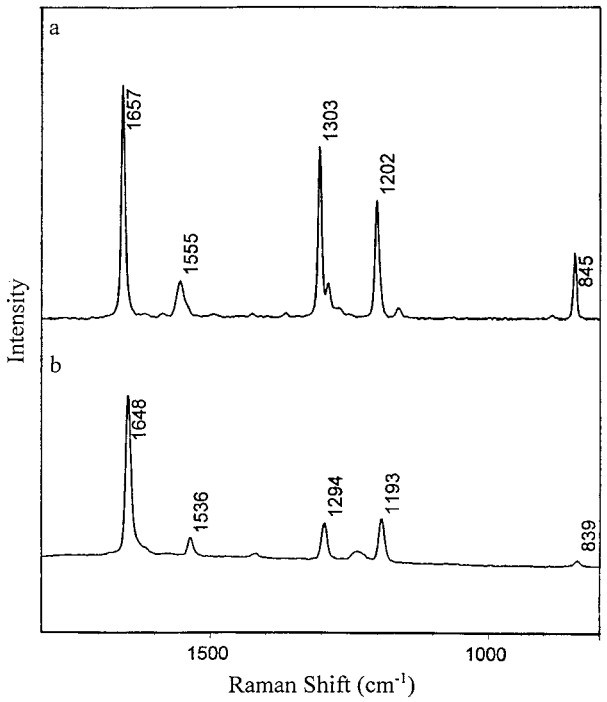

Figure 3. FT-Raman spectra of MV: (a) solid sample and (b) adsorbed on the roughened Ag electrode.

conclude that the surface defects and aggregates of the Ag nanoparticles on the surface of the roughened Ag electrode provide the active sites for the adsorption of MV^{2+}, whereas the isolated silver particles on the surface of the AAgNP/ITO electrode may not possess necessary active sites for the parallel adsorption of MV molecules. This is in parallel to the conclusions of SERS studies of rhodamine 6G with very low concentration reported by Nie and co-workers[27] and Hildebrandt and co-workers,[28] who demonstrated respectively that each colloidal particle contains average of only 3.3 adsorption sites that are especially efficient for the enhancement of Raman scattering. It should also be emphasized that the other possible factors that may affect the adsorption behavior of MV include the embedded and/or coadsorbed Cl^- anions particularly formed during the electrochemical roughening procedure, because the surface of the Ag electrode was roughened in a KCl solution. As shown by Hildebrandt and co-workers[28] and Kiefer and co-workers,[29] surface adsorbed anions provide special active sites to promote the formation of surface complexes, which give additional enhancement factor of rhodamine 6G Raman scattering. However, in the present study, an additional FT-SERS experiment with the AAgNP/ITO electrode in a solution containing 1×10^{-4} M Cl^- anion indicated that the intensities of the Raman bands of adsorbed MV^{2+} on the AAgNP/ITO electrode only slightly increased. Thus, the presence of anions on the surface is not the dominant factor to determine the adsorption of MV in the present case.

To avoid such multipoint or planar adsorption requirement as in the case of MV, PATP was further selected to determine to surface properties of the electrodes. Figure 4 displays the normal FT-Raman spectrum of solid PATP and FT-SERS spectra of PATP on the surfaces of the AAgNP/ITO and roughened Ag electrodes. The solid spectrum (Figure 4a) is similar to that obtain with 514.5 nm excitation as reported by Osawa et al.,[30] except for slight differences in frequency for a few bands. The noticeable differences in the FT-SERS spectrum obtained on the roughened Ag electrode (Figure 4b), relative to those in the solid spectrum, are frequency shifts for some

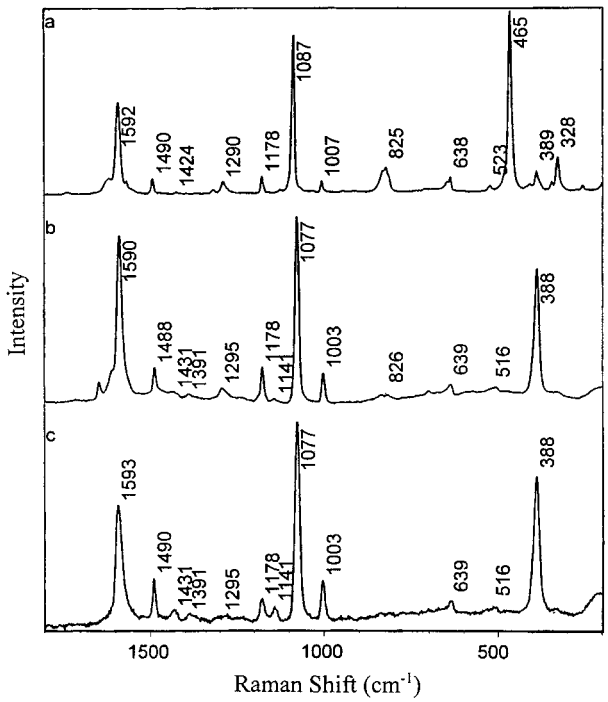

Figure 4. Raman spectra of PATP: (a) solid sample, (b) adsorbed on the roughened Ag electrode, and (c) adsorbed on the AAgNP/ITO electrode.

bands and changes in relative intensity. The band, νCS, shifts from 1086 cm^{-1} in Figure 4a to 1078 cm^{-1} in Figure 4b, and a change in the intensity relative to the band at 1590 cm^{-1} was also observed. This indicates that thiol group in PATP directly contacts with the electrode surface by forming a strong chemical bond. Marked changes also occur in the low-frequency region. The most intense band at 465 cm^{-1} in Figure 4a completely disappears in Figure 4b, whereas a new band appears at 387 cm^{-1} in the FT-SERS spectrum. The band at 465 cm^{-1} previously assigned to the bending mode, γCCC, is not expected to give a large frequency shift upon the adsorption of PATP on the electrode surface. However, a very weak band at 388 cm^{-1}, which was unassigned by Osawa et al.,[30] can be clearly seen in Figure 4a. On the basis of the fact that this band is enhanced upon the adsorption of PATP on the electrode surface, it may be reasonable to assign this band to one of the vibrational modes of the C−S bond, most likely the bending mode of the C−S bond. A similar band was also observed in the SERS spectrum of 2-aminothiophenol.[31]

It should be pointed out that there is significant difference between the FT-SERS spectrum in the present study and the SERS spectrum obtained with the excitation in the visible region. Osawa et al.[30] showed that the b_2 modes at 1573, 1440, 1391, 1142, and 1077 cm^{-1} were dominant in the SERS spectrum obtained with 514 nm excitation, whereas in the present case, the dominant bands are the a_1 vibrational modes, such as νCC at 1591 cm^{-1} and νCS at 1078 cm^{-1}. Nevertheless, in Figure 4b, it is noteworthy that the b_2 modes located at 1436, 1389, and 1143 cm^{-1} are also apparently enhanced. The dramatic selective enhancement of those nontotally symmetric b_2 modes with visible excitation was interpreted in terms of a metal-to-molecule charge transfer (CT) mechanism, which largely depends on the energy of excitation lights and/or applied electrode potential.[7−9,32] Accordingly, the obvious enhancement for the bands of b_2 modes in Figure 4b along with the large frequency shifts and increases in intensities of the bands associated with the C−S bond are indicative of the contribution from CT mechanism. Because a 1064 nm laser was used as the excitation source, a lesser extent of contribution of the Herzberg−Teller term is expected, and thereby, the enhancement of b_2 modes is also less than that with the excitation in the visible region. Furthermore, the enhancement of b_2 modes, relative to a_2 modes, also means that the ring plane of adsorbed PATP molecules is perpendicular to the electrode surface, according to the surface selection rule.[33−37] Thus, PATP is attached to the metal surface just through its sulfur atom, which may only require a single active adsorption site. The predominance of a_1 modes in the FT-SERS spectrum (Figure 4b), on the other hand, may imply that the enhancement via an EM mechanism cannot be neglected. As predicted by Moskovits and co-workers,[33] the totally symmetric vibrational a_1 modes are the most enhanced spectral feature relative to others, when the excitation is at the long wavelength side to the surface plasmon resonance of silver metal.

The spectrum obtained on the AAgNP/ITO surface (Figure 4c) is quite similar to that on the roughened Ag electrode. This reveals that PATP adopts a similar orientation on the surface of the Ag nanoparticles on the AAgNP/ITO electrode. In other words, the surface of the Ag nanoparticles on the AAgNP/ITO electrode also possesses active sties for PATP adsorption, because fewer amounts of active sites are required for the PATP adsorption relative to that for MV. Nevertheless, a few differences for some bands in the two spectra were still observed. Relative intensity remarkably decreases for the band νCC, along with a slight frequency shift from 1590 cm^{-1} on the roughened Ag electrode to 1593 cm^{-1} on the AAgNP/ITO electrode. This band belongs to an a_1 mode, which is composed of a linear combination of three diagonal elements of Raman tensors, α_{xx}, α_{yy}, and α_{zz}, and thereby, changes in this mode do not necessary mean an alteration of the orientation of adsorbed PATP on the surface of the AAgNP/ITO electrode. However, changes in the relative intensity and frequency of a_1 modes do definitely imply changes of the Raman tensor on the direction normal to the surface or local electric field change along this direction.[34] A possible explanation here may arise from a slightly tilted orientation of PATP with respect to the normal of the metal surface and the difference in surface chemical properties of the electrodes. The tilted orientation of PATP, which brings on a interaction between the C−C bond and metal surface, could be a result of lower surface density of the adsorbed PATP compared to that on roughened Ag electrode; therefore, a lesser extent of interaction between adsorbed molecules is expected. In addition, the disappearance of the band at 1620 cm^{-1} could also be a support for the tilted orientation of the adsorbed PATP. This band is most likely from the in-plane vibration mode of $-NH_2$. The difference in chemical properties is supported by the fact that the relative intensities of b_2 modes in Figure 4c increased, compared to those in Figure 4b. Thus, a greater extent of charge transfer from the silver metal to PATP occurs on the AAgNP/ITO electrode. This argument may certainly be understood in terms of free electron distribution in both electrodes. In the case of the roughened Ag electrode, the free electrons are delocalized not only in the Ag nanoparticles on the surface but also in metal bulk, whereas they are confined in the isolated nanostructured Ag particles on the AAgNP/ITO electrode. Therefore, higher electron density is expected in the Ag particles on the AAgNP/ITO electrode, and a greater extent of charge density may be distributed to the adsorbed PATP molecule.

Conclusions

We have demonstrated the difference in surface properties of the AAgNP/ITO and roughened Ag electrodes. On the surface

of the roughened Ag electrode, the strongly adsorbed MV molecules adopt a planar orientation, which requires the active sites formed by aggregation of the nanoparticles and surface defects. Those are lacking on the AAgNP/ITO electrode, where most of the nanoparticles exist independently in the two-dimensional submonolayer structure. The FT-SERS spectra for PATP, on the other hand, show similar spectral features on both of the electrodes, suggesting both of the electrodes can provide the active sites for the adsorption of PATP with similar orientation. The difference in relative intensities of the a_1 modes along with more intense b_2 modes for the AAgNP/ITO electrode are ascribed to a possible tilted orientation of PATP and the difference in surface chemical property relative to that of the roughened Ag electrode.

Acknowledgment. Financial supports from Nature Science Foundation of China (No. 20073028) and Suzhou University are grateful.

References and Notes

(1) Mulvaney, S. P.; Keating, C. D. *Anal. Chem.* **2000,** *72*, 145R.
(2) Kneipp, K.; Kneipp, H.; Itzkan, I.; Dasari, R. R.; Feld, M. S. *Chem. Rev.* **1999**, *99*, 2957.
(3) Brolo, A. G.; Irish, D. E.; Smith, B. D. *J. Mol. Struct*. **1997**, *405*, 29.
(4) Cotton, T. M.; Kim, J. H.; Holt, R. E. *Adv. Biophys. Chem.* **1992**, *2*, 115.
(5) Birke, R. L.; Lu, T.; Lombardi, J. R. *Technical Characteristics of Electrodes and Electrochemical Processes*; Vaema, R.; Selman, J. R., Eds.; Wiley: New York, 1991.
(6) Moskkovits, M. *Rev. Mod. Phys*. **1985**, *57*, 783.
(7) Vo-dinh, T. *Trends Anal. Chem.* **1998**, *17*, 557.
(8) Otta, A. *J. Raman Spectrosc.* **1991**, *22*, 743.
(9) Campion, A.; Kambhampati, P. *Chem. Soc. Rev.* **1998**, *27*, 241.
(10) Shirtcliffe, N.; Nickel, U.; Schneider, S. *J. Colloid Interface Sci.* **1999**, *211*, 122.
(11) Norrod, K. L.; Sundnik, L. M.; Rousell, D.; Rowlen, K. L. *Appl. Spectrosc.* **1997**, *51*, 994.
(12) Emory, S. R.; Haskins, W. E.; Nie, S. *J. Am. Chem. Soc.* **1998**, *120*, 8009.
(13) Sutherland, W. S.; Winefordner, J. D. *J. Raman Spectrosc.* **1991**, *22*, 541.
(14) Rodger, C.; Smith, W. E.; Dent, G.; Edmondson, M. *J. Chem. Soc., Dalton Trans.* **1996**, 5, 791.
(15) Lacy, W. B.; Olson, L. G.; Harris, J. M. *Anal. Chem.* **1999**, *71*, 596.
(16) Bright, R. M.; Musick, M. D.; Natan, M. J. *Langmuir* **1998**, *14*, 5695.
(17) Grabar, K. C.; Griffith, R.; Hommer, M. B.; Natan, M. D. *Anal. Chem.* **1995**, *67*, 735.
(18) Chumanov, G.; Sukolov, K.; Gregory, B. W.; Cotton, T. M. *J. Phys. Chem.* **1996**, *99*, 9466.
(19) Sukolov, K.; Chumanov, G.; Cotton, T. M. *Anal. Chem.* **1998**, *70*, 3898.
(20) Lee, P. C.; Meisel, D. *J. Phys. Chem.* **1982**, *86*, 3391.
(21) Qiao, F.; Wayne, Y.; Cotton, T. M. *J. Phys. Chem*. **1990**, *94*, 2082.
(22) Lu, T.; Birke, R. L.; Lambardi, J. R. *Langmuir* **1986**, *2*, 305.
(23) Lee, P. C.; Schmidt, K.; Gorden, S.; Meisel, D. *Chem. Phys. Lett.* **1981**, *80*, 242.
(24) Forster, M.; Girling, R. B.; Hester, R. E. *J. Raman Spectrosc.* **1982**, *12*, 36.
(25) Grabhorn, H.; Otto, A. *Vacuum* **1990**, *41*, 473.
(26) Zhong, F.; Sun, X.; Wu, G. *J. Mol. Struct.* **1993**, *298*, 55.
(27) Nie, S.; Emory, S. R. *Science* **1997**, *275*, 1102.
(28) Hildebrandt, P.; Stockberger, M. *J. Phys. Chem*. **1984**, *88*, 5935.
(29) Kneipp, K.; Roth, E.; Engert, C.; Kiefer, W. *Chem. Phys. Lett* **1993**, *207*, 450.
(30) Osawa, M.; Matsuda, N.; Yoshll, K.; Uchida, I. *J. Phys. Chem.* **1994**, *98*, 12702.
(31) Griffith, W. P.; Koh, T. Y. *Spectrochim. Acta* **1995**, *51*, 253.
(32) Lambardi, J. R.; Birke, R. L.; Lu, T.; Xu, J. *J. Chem. Phys*. **1986**, *84*, 4171.
(33) Moskovits, M.; Suh, J. S. *J. Phys. Chem.* **1984**, *88*, 5526.
(34) Carron, K. T.; Hurley, L. G. *J. Phys. Chem.* **1991**, *95*, 9979.
(35) Pagannone, M.; Fornari, B.; Mattei, G. *Spectrochim. Acta* **1987**, *43*A, 621.
(36) Takahashi, M.; Furukawa, H.; Fujita, M.; Ito, M. *J. Phys. Chem.* **1987**, *91*, 9540.
(37) Creighton, J. A. *Surf. Sci.* **1986**, *173*, 665.